INCORPORATION OF STEREO, REGIO AND COMONOMER DEFECTS INTO THE CRYSTALLINE REGIONS OF ISOTACTIC POLYPROPYLENE: RESULTS FROM NMR, MOLECULAR DYNAMICS AND CHEMICAL SHIFT CALCULATIONS

D.L. VanderHart and M.R. Nyden
National Institute of Standards and Technology
Gaithersburg, MD 20899
and
R.G. Alamo
Department of Chemical Engineering
FAMU-FSU
Tallahassee, FL 32310-6046
And
L. Mandelkern
Department of Chemistry
FSU
Tallahassee, FL 32306

Introduction

The concentrations of normally occurring stereo and regio defects in isotactic polypropylene (iPP) influence properties. This influence mainly arises because defects are discriminated against during the formation of crystallites; hence, sufficient numbers of defects can reduce crystallinity,[1] crystal thickness[2] and melting point[3]. These defects are introduced into the iPP chains during polymerization, and, especially because of the development of varied metallocene catalysts[4] for homogeneous polymerization of iPP, one can obtain samples for study where these defects both vary in relative concentration and are quite randomly distributed throughout all of the iPP chains. In this report we take advantage of ^{13}C NMR methods that allow us both to isolate that portion of the signal which arises from carbons in the crystalline(CR) regions of the sample and to identify (and integrate) suites of new resonances which can be associated with different types of defects.

The types of defects which will be discussed here include stereo-mrrm[5], regio-2,1-erythro[5], ethylene comonomer and butylene comonomer. The sample-average defect concentration for each defect is measureable[1, 6-10] and, for our samples, has been measured via solution-state NMR. The **stereo-mrrm** defect (referring to basic "m" (meso) and "r" (racemic) dyad nomenclature[5]) defines a pentad (5-residue) stereosequence where the methyl and proton substituents on the asymmetric carbon of the central residue are switched with respect to the ideal mmmm stereosequence of the iPP chain. The mrrm pentad defines the simplest, and the most common type of stereo defect[11]. Other, more complicated types of stereo defects, involving errors at more than one repeat unit, are generally also present in minor amounts. In contrast to stereo defects which preserve the head-to-tail character of olefin addition, regio defects disrupt this character. Head-head (or '2,1', as opposed to the normal '1,2') polymerization describes one type of regio defect. We will investigate the "**regio 2,1-erythro**" defect where, at the head-to-head position, the 2 methyl groups lie on the same side of the zigzag plane when the backbone is extended in to the all-trans conformation.

Finally, we will also consider defects associated with vinyl comonomers, specifically ethylene and butylene. One might anticipate that the ethylene repeat unit could easily replace the propylene unit in the CR lattice since the former is smaller; furthermore, the butylene repeat unit could be more strongly rejected on the basis of its larger size. Assuming, as a first approximation, that the concentration of a given defect, C_{CR}(def), in the CR regions is proportional to the sample-wide average concentration, C_{Ave}(def), of that same defect, we will define the 'crystalline partitioning coefficient', P_{CR}(def), for that defect by the relationship:

$$P_{CR}(\text{def}) = C_{CR}(\text{def})/ C_{Ave}(\text{def}). \quad (1)$$

It is a main objective of this paper to establish P_{CR} values for the stereo-mrrm, regio 2,1 erythro, ethylene-comonomer and butylene-comonomer defects. Since C_{Ave}(def) is known from solution NMR, only C_{CR}(def) values need be determined. In order to do that, we must be able to assign properly the number of carbons per defect which contribute to each new, integrable resonance belonging to that defect. We emphasize that a knowledge of the solution-state resonance positions for carbons at or near defects is not very relevant to this critical assignment problem since a) defect segments in the CR lattice will likely adopt only one, or possibly two, conformations of minimum energy instead of experiencing an average over all available conformations as happens in solution, b) minimum-energy conformations in the CR lattice may strongly deviate from minimum-energy conformations in solution since intermolecular potentials are fixed in the CR lattice, and c) chemical shifts are very conformationally dependent.[12] In our attempt to make proper assignments for defect resonances, we performed molecular dynamics calculations, including a 'thermal annealing cycle', in order to minimize conformational energy in the CR lattice. Following this, *ab initio* chemical shift calculations were performed on a methyl-terminated oligomeric fragment containing this defect. The geometry of this oligomer was extracted from the preceding calculation.

Experimental

The NMR method[13] for separating the signals from the CR and the NC regions is based on differences in the intrinsic rotating frame proton relaxation times in the 2 regions. Hence, using 2 different spin locking[14] (SL) times preceding cross polarization[15] (CP), one can obtain spectra having different relative weighting of the signals from the CR and NC regions. One can then take linear combinations of these spectra in order to isolate what we refer to as the 'CR' and 'NC' spectra. Spectra obtained in this way have 2 characteristics, namely, that a) the weak signals from carbons at defects are separated into CR and NC contributions to the same degree of precision as the strong signals from the abundant non-defect carbons are separated (This is true even if the local molecular mobility near a defect may change somewhat.) and b) owing to proton spin diffusion,[16] the separation of the strong, non-defect carbon signals is not perfect…there is some distortion. For both the NC and the CR spectra, the signal contributions are stronger from the interior of the region and weaker from the interface region. Moreover, there is also a minor positive contribution from carbons near the interface in the unwanted region; these contributions are offset by a negative contribution from the interior of the unwanted region. These non-idealities in the weighting of signals arising from carbons in different morphological locations are a nuisance in the sense that the apparent, measured concentration of defects, say, in the CR region will only be accurate if the concentration of defects is uniform throughout each of the regions. On the other hand, the non-idealities mentioned allow us to address the question whether there is a high concentration of defects at the interface since the non-ideality predicts that signals from such defects should appear in both the CR and the NC spectra.

The non-commercial NMR spectrometer used in this investigation operates at 2.35 T (25.2 MHz). Magic angle spinning[17] (MAS) was employed in a non-commercial probe which incorporated a 7-mm-OD rotor/stator combination manufactured by Doty Scientific, Inc.[18] All carbon signals were generated via CP. All pulse sequences consisted of a proton SL period (SL times were 0 ms or a SL time in the 6 ms to 8 ms range) followed immediately by a 0.7-ms CP time. Radiofrequency field strengths used correspond to nutation frequencies of 62 and 66 kHz for protons and ^{13}C nuclei, respectively. MAS frequency was uniformly set to 4.0 kHz. Delay times between experiments were 4 s to 5 s and 20,000 to 100,000 scans were taken in order to generate adequate signal-to-noise.

Most of the isotactic polypropylene (iPP) samples were experimental materials obtained from manufacturers of iPP's. All but one sample have been synthesized using homogeneous metallocene catalysts. The unique sample is a so-called psuedo-fraction of an iPP polymerized with a heterogeneous Ziegler-Natta catalyst. This fraction was isolated by partial crystallization in dilute toluene; this process lowers the concentration of the non-crystallizable chains that have defect contents well above that predicted by the sample-average defect level. The nomenclature (of the form "Xiii-jjjY") we adopt for these samples contains 4 pieces of information. 'X' is either 'M' (metallocene catalyst) or 'Z' (Ziegler-Natta catalyst). 'iii' is the molecular mass in kg/mol. 'jjj' is the total defect level, expressed as (100 x number of defect residues)/(total number of residues). Finally, 'Y' is the dominant type of defect ('S' for stereo-mrrm, 'R2' for regio, 2,1, 'E' for ethylene comonomer, and 'B' for butylene-comonomer). In order to prepare each sample under comparable conditions, each sample was melt-crystallized during a cooling cycle controlled at 1°C/min. Given that the kinetics of crystallization could, in principle, be important for establishing the partitioning of defects, we felt this crystallization history, rather than some isothermal history, would be less kinetics-sensitive, given that the level of defects influence melting points (and undercoolings).

Solution-state **^{13}C** NMR spectra were run at 7.05 T. Spectra were run at 125°C in 10 mm tubes using 15-mass-percent solutions. Average defect levels were established based on published assignments.[1, 6-10]

Results and Discussion

In Figure 1 we show vertically amplified spectra of the CR component for four metallocene-polymerized iPP samples. These samples are each dominated by a different defect so these spectra illustrate the different patterns associated with each type of defect. At least one other sample with a lower concentration of each of the same types of defects was also studied in order to support the association of a given group of resonances with each particular defect. The relative intensity of any particular defect resonance, within the signal to noise, was proportional to the overall concentration of that defect for all of the metallocene-polymerized samples.

In Figure 1, the 3 resonances associated with the defect-free iPP chain are illustrated in the bottom spectrum; these resonances consist of the methyl, methine and methylene resonances at 22.1 ppm, 26.7 ppm and 44.0 ppm, respectively. Each weak resonance associated with the dominant defect in each of the four samples is indicated by an asterisk in Figure 1. For the regio-2,1-erythro defect, there is a suite of 4 new defect resonances. For the stereo-mrrm defect there are 5 identifiable new resonances. For the butylene-comonomer, 4 new resonances appear including a rather intense, relatively broad resonance near 39 ppm and a very broad methyl resonance. Finally, for the ethylene- comonomer, 3 new defect-related resonances appear.

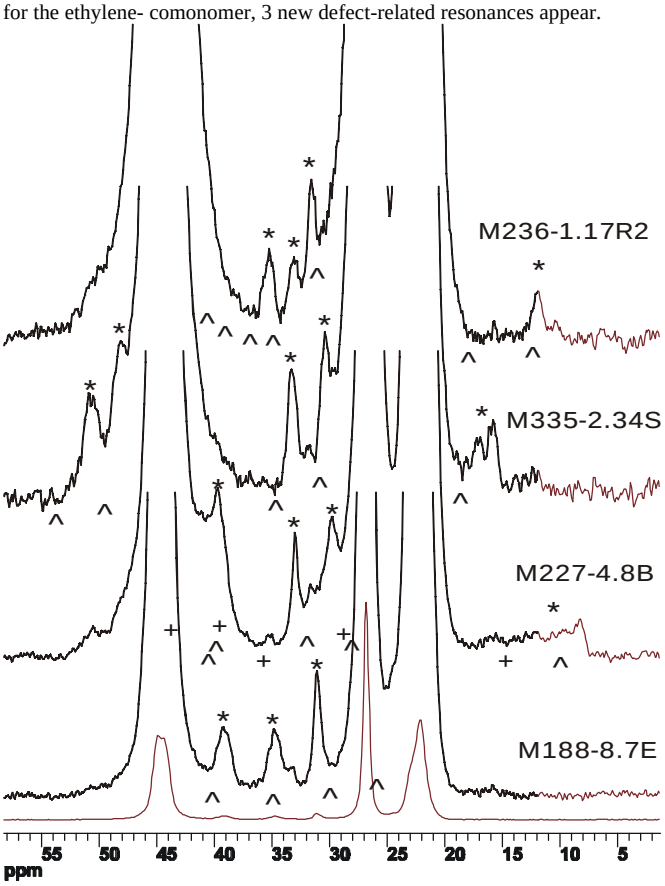

Figure 1. Spectra of the CR regions of the indicated iPP's, each of which is dominated by a different type of defect. From the top down, the dominant defects are: regio-2,1-erythro, stereo-mrrm, butylene-comonomer and ethylene-comonomer. The bottom spectrum is that of the M188-8.7E sample, scaled down by a factor of 20. Asterisks appear above each of the defect resonances which are assigned to each dominant defect. The '^' symbol is placed at the chemical shifts predicted from lattice-energy minimization followed by *ab initio* chemical shift calculations. For the M227-4.8B sample, both '^' and '+' symbols are used to indicate those calculated values which belong to 2 distinct conformers that we believe to be contributing to the defect spectrum. Main-peak scaling varies in order to highlight defect resonances.

The intensities of the defect resonances, relative to the intensities of the main resonances convey the information about the concentration of defects in the CR regions. However, the samples associated with each of the spectra in Figure 1 are each contaminated by some level of other types of defects and minor resonances associated with these other defects are seen in all spectra in Figure 1 except that of the M236-1.17R2 sample. In Table 1, a summary of the different defect contributions is given for each of these samples. Before evaluating the integrals associated with the dominant defects in these CR spectra, appropriate portions of other CR spectra were subtracted to correct for the presence of the contaminating defects; this correction presumes that all effects are additive.

Table 1. Summary of Average Defect Contents (mol fraction) for the iPP Samples of Figure 1. Standard uncertainties are given in parentheses in units of the last significant figure.

Sample	Stereo-mrrm	Regio-2,1-Erythro	Regio-2,1-Threo	Como-nomer	Other[a]
M335-2.34S	.0143(4)	.0023(1)	.0030(2)	------	.0038(4)
M236-1.17R2		.0095(6)	------	------	.0022(6)
M188-8.7E	.0060(6)	.0040(6)		.0750(9) (Eth)	.0020(6)
M227-4.8B	.0067(6)	.0070(8)	------	.0320(7) (But)	.0023(6)

a) Includes non-mrrm stereo defects and 1,3 regio defects, the latter being the insertion of a sequence of 3 consecutive methylene groups into the backbone.

Computations aimed at defining the minimum-energy conformation for a given defect were performed using the Discover 95[18] software with the Centralized Valence Force Field. All computations used the α-crystal lattice[19,20] in which 26 stems of 21-repeat-unit length were employed. A defect was placed in the middle of a stem centered in the lattice. This stem along with its nearest neighbor plus the full array of next nearest neighbors was allowed to move in the simulation. The outer perimeter of 16 stems remained fixed to preserve the general structure of the lattice. Cycles of simulated thermal annealing were performed and from the resulting energy-minimized conformation defining the 'defect' stem, a central section, 7.5 or 8.5 repeat units long, was excised. Protons were added to the methylene terminae of these sections, thus forming a methyl-terminated oligomer containing the defect with an energy-minimized conformation. Chemical shift calculations, using Gaussian 98 software[21] and a choice of computation at the BLYP 6-311+G(2d,p) level, were then performed. When applicable, computations were performed on both defect-containing and defect-free chains. Then the differences in computed shifts for corresponding carbons were used as the "calculated shifts". Most of the computed values indicated in Figure 1 are based on these computed differences for each carbon type.

The computed shifts included in Figure 1 are those which show deviations greater than 2 ppm from the defect-free chain. While it is difficult to evaluate the accuracy of the shift calculations, we regard the differences just described to have expanded uncertainties of 2 ppm to 3 ppm, while the absolute values calculated have considerably less accuracy. This is why others[22-24] who do these calculations have used linear correlations to convert calculated shifts into predicted shifts. In fact, considering stems which contain either the regio-2,1-erythro defect or the butylene defect, there are 2 carbons on each of these stems which have no analogous carbons on the defect-free chain; hence, we also used linear correlations to predict the chemcal shift for each of these carbons. In order to claim reasonable agreement with experiment, it is clear that the positions of some of the calculated resonances must correspond to defect resonances that are actually submerged beneath the main resonances. At this point, we are quite satisfied with the agreement of the calculated values, except for the regio 2,1-erythro defect. Table 2 summarizes the partitioning coefficient and some geometric information for each defect type, based on the relative intensity information in the CR spectra and based on the assignment/conformational information deduced from the energy-minimization/chemical-shift calculations. For reference, we define the normal sequence of dihedral angles for the defect-free, 3_1 helical chains to be (..g^+t g^+t g^+t..) where 'g' stands for 'gauche' (either g^+ or g^-) and 't' for 'trans'.

Table 2. Partitioning Coefficients, Approximate Sequence of Dihedral Angles and Our Confidence Level that the Computations Have Identified the Assignment/Geometry Associated with these 4 Types of Defects in Crystalline iPP.

Defect Type	P_{CR}[a]	Dihedral Angle Sequence	Confidence Level
Regio 2,1 erythro	0.28(8)	(..$g^+t\,g^-ttt\,g^+t$..)	Fair
Stereo-mrrm	0.48(6)	(..$g^+ttt\,g^-t\,g^+t$..)	Good
Butylene comonomer	0.52(8)	(..$g^+t\ \ g^+t\ \ g^+t$..) &(..$g^+t\,g^+t\,g^+t$..)	Good
Ethylene comonomer	0.40(4)	(..$g^+t\,g^+t\,g^+t$..)	Excellent

a) Standard uncertainties are given in parentheses in units of the least significant digit. Uncertainties reflect uncertainties only in evaluating defect-related integrals; only for the regio defect are ambiguities related to assignment included.

b) Two conformers appear to be populated for the butylene-comonomer defect. Both preserve the 3_1 helix; they differ in that the methyl of the ethyl branch is either 't' and 'g' or 'g' and 'g' to the 2 backbone CH_2's.

Conclusion

We have shown that under conditions of crystallization during cooling at 1°C/min, substantial amounts of 'defects' of the types a) stereo-mrrm, b) regio-2,1-erythro, c) ethylene-comonomer and d) butylene-comonomer can be found in the crystalline regions, the regio defect being most strongly rejected. We have also shown that the important resonance-assignment question can be addressed using computational approaches for 1) finding minimum-energy conformations in the crystal lattice and 2) doing *ab initio* chemical shift calculations to predict spectra associated with the defects. From the agreement in shifts between calculation and experiment we can also argue for certain general conformations near these defects. A corollary finding, not discussed above is that the one Ziegler-Natta pseudo-fraction, whose defect population was mainly stereo-mrrm, displayed a P_{CR} value significantly less than a correponding metallocene iPP. We took this as support for the non-uniform distribution of defects/per/chain in Ziegler-Natta iPP's. Also, not discussed above is the conclusion that these defects are not highly concentrated on the CR side of the CR/NC interface owing to the absence of these resonances in the spectra of the NC region. (At the same time, we obtain no information about the possibility that defects concentrate on the NC side of that interface. This follows from the fact that, at ambient temperature, defect resonances in the NC region are quite broad and cannot be separately identified against the background of the intense resonances of the non-defect carbons.) The different partitioning coefficients add another dimension to the control of iPP properties via a tailoring of defect concentrations. The direct evidence of the inclusion of defects in the crystalline lattice of iPP-based homopolymers and random copolymers leads to a reevaluation of the determination of the degree of crystallinity from heat of fusion measurements by DSC. It is anticipated that the heat of fusion per mol of crystalline sample is a function of the concentration and type of defect in the crystalline region. It is interesting that the larger butylene comonomer is more accepted into the iPP lattice than is the smaller ethylene comonomer.

Acknowledgement

The authors wish to thank Dr. J. C. Randall of Exxon for stimulating and valuable discussions as well as assistance in the analysis of the high resolution NMR data. R.G.A. acknowledges support of this work by the National Science Foundation, Polymer Program (DMR-9753258).

References

(1) Isasi, J.R.; L. Mandelkern; Galante, M.J.; Alamo, R.G.;*J. Polym. Sci. B: Polym. Phys*. 1999, *37*, 323.
(2) Cheng, S.Z.D.; Jnimak, J.J.; Zhang, A.; Hsieh, E.T. *Polymer* 1991, *32*, 648.
(3) Cheng, S.Z.D.; Jnimak, J.J.; Zhang, A.; Hsieh, E.T. *Polymer* 1992, *33*, 728.
(4) Brintzinger, H.H.; Fischer, D.; Mülhaupt, R.; Rieger, B.; Waymouth, R.M. *Angew. Chem. Int. Ed. Engl*.1995, *34*, 1143.
(5) Randall, J.C. "*Polymer Sequence Determination: Carbon-13 NMR Method*", Academic Press, New York, 1977, Chap. 1.
(6) Zambelli, A.; Locatelli, P.; Bajo, G.; Bovey, F.A. *Macromolecules* 1975, *5*, 687.
(7) Hayashi, T.; Inoue, Y.; Chûjô, R.; Asakura, T. *Polymer* 1988, *29*, 138.
(8) Soga, K.; Shiono, T. *Makromol. Chem. Rapid Commun*. 1987, *8*, 305.
(9) Grassi, A.; Zambelli, A.; Resconi, L.; Albizzati, E.; Mazzocchi, R. *Macromolecules* 1988, *21*, 617.
(10) Busico, V.; Cipullo, R.; Chadwick, J.C.; Modder, J.F.; Sudmeijer, O. Macromolecules 1994, 27, 7538.
(11) Randall, J.C. *Macromolecules* 1997, *30*, 803.
(12) Belfiore, L.A.; Schilling, F.C.; Tonelli, A.E.; Lovinger, A; Bovey, F.A. *Macromolecules*1984, *17*, 2561.
(13) VanderHart, D.L.; Pérez, E. *Macromolecules* 1986, *19*, 1902.
(14) Solomon, I. *C.R. Acad. Sci*.1959, *248*, 92.
(15) Hartmann, S.R.; Hahn, E.L. *Phys. Rev*. 1962, *128*, 2042.
(16) "*The Principles of Nuclear Magnetism*", Abragam, A., Oxford University Press, 1961, Chap. V.
(17) Lowe, I.J. *Phys. Rev. Lett*. 1959, *2*, 85.
(18) Certain commercial companies are named in order to specify adequately the experimental procedure. This is no way implies endorsement or recommendation by the authors or their agencies.
(19) Natta, G.; Corradini, P. *Suppl. Nuovo Cimento* 1960, *15*, 40.
(20) Hikosaka, M.; Seto, T. *Polymer J*. 1973, *5*, 111.
(21) Gaussian 98 (Revision A.2), M. J. Frisch, G. W. Trucks, H. B. Schlegel, G. E. Scuseria, M.A.Robb, J. R. Cheeseman, V. G. Zakrzewski, J. A. Montgomery, R. E. Stratmann, J. C. Burant, S.Dapprich, J. M. Millam, A. D. Daniels, K. N. Kudin, M. C. Strain, O. Farkas, J. Tomasi, V.Barone, M. Cossi, R. Cammi, B. Mennucci, C. Pomelli, C. Adamo, S. Clifford, J. Ochterski, G.A. Petersson, P. Y. Ayala, Q. Cui, K. Morokuma, D. K. Malick, A. D. Rabuck, K. Raghavachari, J. B. Foresman, J. Cioslowski, J. V. Ortiz, B. B. Stefanov, G. Liu, A. Liashenko, P. Piskorz, I. Komaromi, R. Gomperts, R. L. Martin, D. J. Fox, T. Keith, M. A. Al-Laham, C. Y. Peng, A. Nanayakkara, C. Gonzalez, M. Challacombe, P. M. W. Gill, B. G. Johnson, W. Chen, M. W. Wong, J. L. Andres, M. Head-Gordon, E. S. Replogle and J. A. Pople, Gaussian, Inc., Pittsburgh PA (1998).
(22) de Dios, A.C.; Oldfield, E., *J. Am. Chem. Soc.* 1994, *116*, 5307.
(23) Harper, J.K.; McGeorge, G.; Grant, D.M., *Magn. Reson. Chem.* 1998, *36*, S135
(24) Harper, J.K.; McGeorge, G.; Grant, D.M., *J. Am. Chem. Soc.* 1999, *121* 6488.

Citation for this paper:
Abstracts of Papers of the American Chemical Society 2000 Mar 26; 219:48-PMSE.